Proceedings of the
International Conference on Mechanical Engineering 2011
(ICME2011) 18-20 December 2011, Dhaka, Bangladesh

ICME11-FL-025

REYNOLDS NUMBER EFFECT ON FLOW-INDUCED FORCES ON TWO TANDEM CYLINDERS

Md. Mahbub Alam and J.P. Meyer

Department of Mechanical and Aeronautical Engineering University of PretoriaPretoria , South Africa

ABSTRACT

Reynolds number (*Re*) effects on fluctuating lift (C_{Lf}) and drag (C_{Df}) forces and Strouhal numbers (*St*) of the downstream cylinder of two tandem cylinders are investigated experimentally for $Re = 9.7\times10^3 \sim 6.5\times10^4$. The center-to-center spacing ratio (*L/D*) between the cylinders is varied from 1.1 to 4.5 with a step of 0.1, where *D* is the cylinder diameter. The results show that C_{Lf}, C_{Df} and *St* are highly dependent on *Re* in the *Re* range examined for $L/D < 3$. While C_{Lf} and C_{Df} at $L/D = 2.4$ for $Re = 6.5\times10^4$ are about 2 and 2.8 times higher, respectively, than those for a single cylinder, those for $Re = 1.6\times10^4$ are 0.5 and 0.7 times. They are very sensitive to *L/D* for higher *Re* but less for lower *Re*. The associated physics are dug out.

Keywords: Forces, Flow Structures, Strouhal Numbers, Tandem Cylinders, Fluctuating Lift and Drag.

1. INTRODUCTION

Slender structures in groups have many engineering applications, for example, chimney stacks, tube bundles in heat exchangers, cooling of electronic equipments, high-rise buildings, harvesting wave and tide energy from ocean, overhead power-line bundles, bridge piers, stays, masts, chemical-reaction towers and offshore platforms. Naturally, it is important to understand the proximity effect on aerodynamics associated with multiple closely spaced cylindrical structures. Two fluid-dynamically interfering cylinders may be considered as the basic element of multiple structures and the knowledge of this flow is insightful for understanding the flow around more structures. As such, the flow around two cylinders has received a great deal of attention in the literature. There is no doubt that flow physics around two cylinders is much more complex and complicated than that around a single cylinder, because of interference between the cylinders, between the wakes, among four shear layers, etc. The alternate shedding of vortices in the near wake leads to fluctuating forces on the structures and may cause structural vibrations, acoustic noise, or resonance, which in some cases can trigger failure. The study of aerodynamics of two closely separated structures is thus of both fundamental and practical significance. Fluid forces, Strouhal numbers (*St*) and flow structures are the major factors considered in the design of slender structures subjected to a cross-flow.

When a cylinder is placed in-line downstream of another cylinder, it is called a *tandem arrangement*. When two cylinders are placed in tandem, a complex flow structure is generated as a result of mutual interactions among the wakes behind the bodies. Flow around two tandem circular cylinders may be classified into three regimes based on center-to-center spacing *L/D* [1]: (1) an extended-body regime, where *L/D* ranges from 1 to 1.5 and the two cylinders are so close to each other that the free shear layers separated from the upstream cylinder overshoot the downstream one; (2) a reattachment regime, where *L/D* is between 1.5 and 4 (critical *L/D*), and the shear layers reattach on the downstream cylinder; (3) a co-shedding regime, where $L/D \geq$ critical and the shear layers roll up alternately, forming a vortex street in the gap between as well as behind the cylinders. In the co-shedding regime, the frequency of vortex shedding from one cylinder is identical to that from the other [2]. Vortex shedding from the downstream cylinder is triggered by the arrival of vortices generated by the upstream cylinder.

Biermann and Herrnstein [3] measured the combined drag force acting on the two parallel circular cylinders in a tandem arrangement up to $L/D = 8$ ($Re = 1.05\times10^5$). They measured only time-averaged drag (C_D) on the individual cylinders; therefore, more investigation was needed to clarify the other parameters, such as, root-mean-square (fluctuating) drag and lift (C_{Df}, C_{Lf}), Strouhal number (*St*), cylinder surface pressures, wakes, boundary layer characteristics around the cylinders, etc. Time-averaged pressure measurements on the surfaces of the cylinders were conducted by Zdravkovich and Pridden [4] at $Re = 6\times10^4$, and Alam et al. [5] at $Re = 6.5\times10^4$. The results showed that for $L/D < 3.5$ a negative pressure on the front surface of the downstream cylinder

was generated instead of a positive pressure, exceeding that on the rear surface. In case of the upstream cylinder, the pressure only on rear surface was affected by the presence of the downstream cylinder. Nevertheless, beyond L/D = 4, the pressure distribution around the cylinders is comparable to that around a single isolated cylinder. Fluctuating surface pressure, C_{Df}, C_{Lf} and behavior of boundary layer on the cylinders for L/D < 9 were investigated by Alam et al. [5] at $Re = 6.5\times10^4$. In the reattachment regime, they established a correlation between C_{Lf} and reattachment position of the upstream-cylinder shear layers on the downstream cylinder; as the reattachment position moved toward the forward stagnation line, C_{Lf} on the downstream cylinder increased and vice versa.

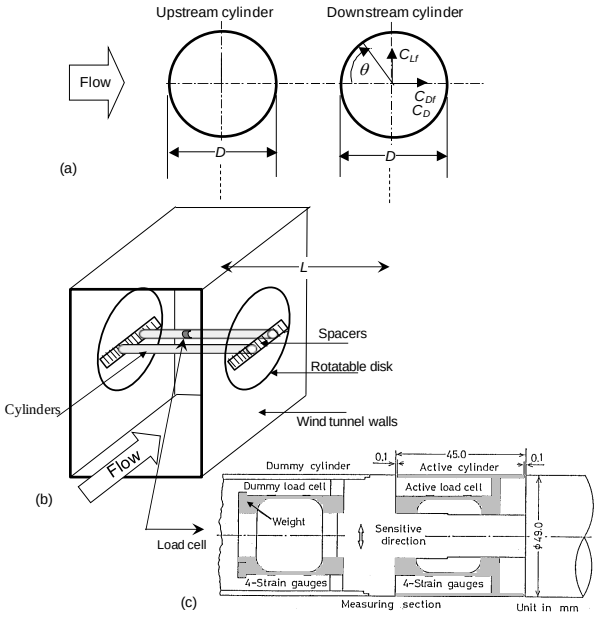

Fig 1. (a) Notation of tandem configuration, (b) a schematic of experimental arrangement, and (c) load cell details.

Igarashi [6] examined the *Re* effects in the wake of two tandem cylinders on *St* and pressure fluctuations for $Re = 8.7\times10^3 \sim 5.2\times10^4$, and noted that, with increasing *Re*, the pressure fluctuation on the cylinder surfaces increased and *St* decreased greatly between $Re = 1\times10^4$ and 4×10^4. Ljungkrona and Sundén's [7] flow visualization and pressure distribution measurements in the wake of two tandem cylinders (L/D= 1.25 ~ 4.0 and $Re = 3.0\times10^3 \sim 4.0\times10^4$) indicated a dependence on *Re* of the critical L/D, at which a bi-stable flow occurred and the shear layers separating from the upstream cylinder changed from reattachment upon the downstream cylinder to the rollup, forming vortices, in the gap of the cylinders. Zdravkovich and Pridden [4] examined *Re* effect on C_D at $Re = 3.1\times10^4 \sim 1.2\times10^5$. When the two cylinders were in contact, C_D on the downstream cylinder was negative, increasing rapidly with L/D. An interruption of the increase rate occurred, forming a 'kink' at $L/D \approx 2.5$. The 'kink' was however absent at $Re \leq 3.1\times10^4$. The physics behind the presence and absence of the 'kink' was left unexplained, with a notation "further research is necessary to clarify this change at small Reynolds numbers".

Previous investigations are in general focused on flow, C_D, *St*, for certain *Re*, barely giving any attention to C_{Df} and C_{Lf} in spite of the fact that the latter is of both fundamental and practical importance in fluid-structure interaction. The objectives of the investigation were to (i) measure *St*, C_{Df} and C_{Lf} on the downstream cylinder, (ii) find their dependences on *Re*, and (iii) get insight into the physics of the dependences including the 'kink'.

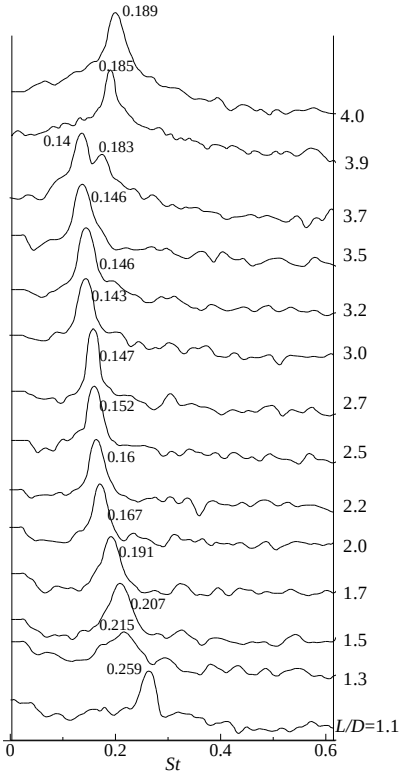

Fig 2. Fourier power spectrum of fluctuating lift on the downstream cylinder at $Re = 9.7\times10^3$.

2. EXPERIMENTAL DETAILS

Measurements were done in a low-speed, closed-circuit wind tunnel with a test section of 1.20 m in height, 0.30 m in width, and 2.2 m in length (Fig 1b). In the test section side walls, two circular holes of 0.5 m diameter, one opposite to the other, were made where two circular disks, each included a slit for cylinders were placed (Fig 1b). The diameter of each cylinder was 49 mm. The cylinders spanned the horizontal 0.3 m dimension of the wind tunnel. *Re* based on cylinder diameter and free-stream velocity was 9.7×10^3, 1.6×10^4, 3.2×10^4, and 6.5×10^4. The turbulent intensity was 0.5%. A fine-mesh honeycomb that was placed at the entrance of the test-section to provide a uniform flow was responsible for generating turbulence. In order to check the spanwise uniformity of flow as well as spanwise separation of flow over a single cylinder for fluid forces being measured by a load cell (which will be discussed next), circumferential time-averaged and fluctuating pressures on the surface of the cylinder at the mid-section, and at ±35 mm and ±80 mm (from the mid-section), were measured. The results showed that the time-averaged and fluctuating pressure distributions at

the five different sections were the same within the accuracy of measurement. The position of a point on the surface of the cylinder is denoted by θ, measured from the front stagnation point.

Fluid forces were measured over a small spanwise length of the cylinders, using load cells (Fig. 1c). The cylinder to be measured was built in with an active ('live') section of a spanwise 45 mm (0.92*D*) length and two dummy sections. This size was determined taking into account the cross-correlation length of fluctuating pressure in the spanwise direction of the cylinder. The active section, placed between the two dummy sections, corresponded to the midspan of the cylinder and was installed with a load cell that consisted of four semiconductor strain gauges. One of the dummy sections was also instrumented with another load cell of the same configuration. The load cell inside the active section measured a combination of fluid forces and forces due to vibration transmitted from outside through the cylinder support, whilst that inside the dummy section measured the latter forces only. Hence the fluid forces acting on the active section could be calculated by subtracting the output of the load cell inside the dummy section from that of the load cell inside the active section. See Alam et al. [9] for details of the load cell.

St was estimated from spectral analysis of the fluctuating lift and flow velocity measured at 2D downstream and D sidewise from the center of the downstream cylinder. Fig 1 is a schematic diagram showing the arrangement of two cylinders, definition of symbols and coordinate systems. *T* is the center-to-center distance between the cylinders. The position of a point on the surface of a cylinder is defined by the azimuth angle θ, measured from the direction of free-stream flow. Experiments were performed for L/D = 1.1 ~ 4.5. Very fine-tuning of L/D = 0.1was adopted.

3. RESULTS AND DISCUSSION

3.1. Strouhal Number and Flow Structures

Power spectra of fluctuating lift are shown in Figs 2-5 at $Re = 9.7\times10^3$, 1.6×10^4, 3.2×10^4 and 6.5×10^4. At $Re = 9.7\times10^3$, *St* drops suddenly from 0.259 to 0.215 between L/D = 1.1 and 1.3 (Fig 2). The drop is connected to change in flow structure from an over-shoot flow (Fig 6a) to rear-side reattachment flow (Fig 6b) which corresponds to *St* of an isolated cylinder value (≈ 0.19). Here, front, front-side, rear-side and rear surfaces correspond to θ = 0° ~ 60°, 60° ~ 90°, 90° ~ 120°, and 120° ~ 180°, respectively. In the reattachment flow, the two shear layers from the upstream cylinder reattach alternately, say in the first half cycle the upper shear layer (Fig $6b_1$) reattaches and in the next half cycle the lower shear layer reattaches (Fig $6b_2$). The rear-side reattachment flow takes place between L/D = 1.3 and 1.7. With increasing L/D, the reattachment point proceeds forward and front-side reattachment therefore occurs for L/D 2.0 ≤ L/D ≤ 3.5 (Fig 6c). The front-side reattachment flow corresponds to a smaller *St* than an isolated cylinder flow. *St* is again about 0.19 for $L/D \geq 3.9$, insinuating a co-shedding flow (Fig 6e). Two peaks are seen at L/D = 3.7, indicating a bi-stable flow between the front-reattachment and co-shedding flows (Fig 6d). This L/D is called as the critical spacing.

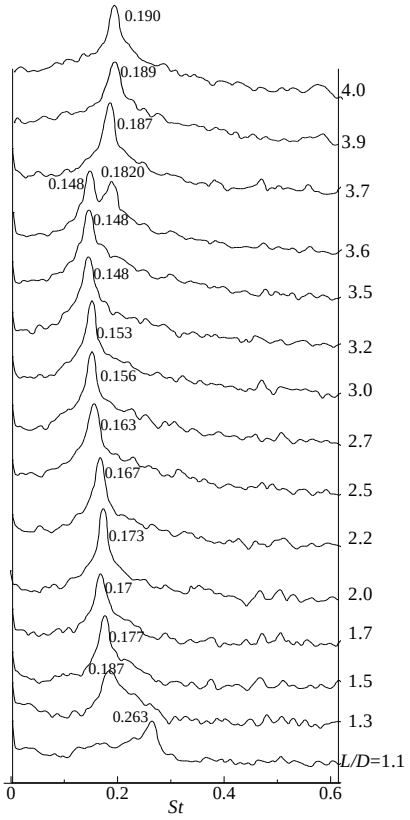

Fig 3. Fourier power spectrum of fluctuating lift on the downstream cylinder at $Re = 1.6\times10^4$.

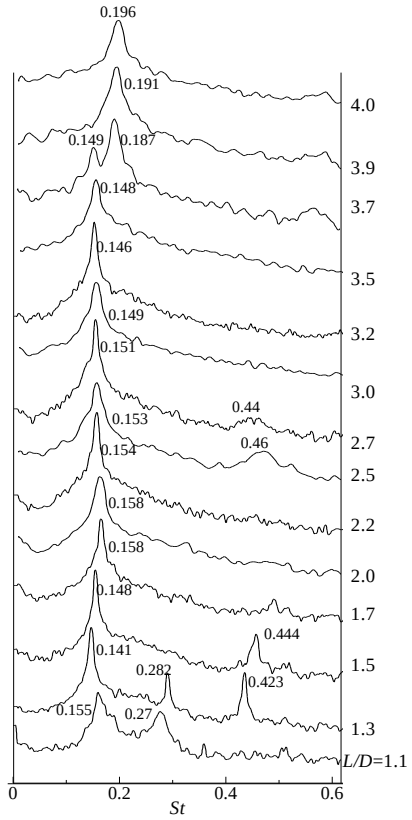

Fig 4. Fourier power spectrum of fluctuating lift on the downstream cylinder at $Re = 3.2\times10^4$.

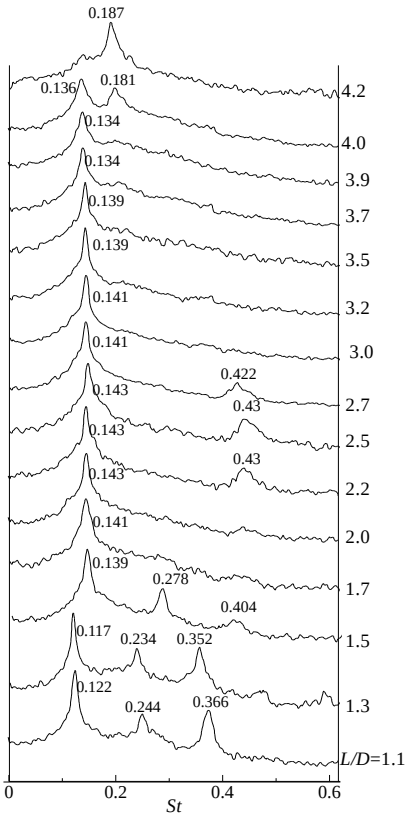

Fig 5. Fourier power spectrum of fluctuating lift on the downstream cylinder at $Re = 6.5\times10^4$.

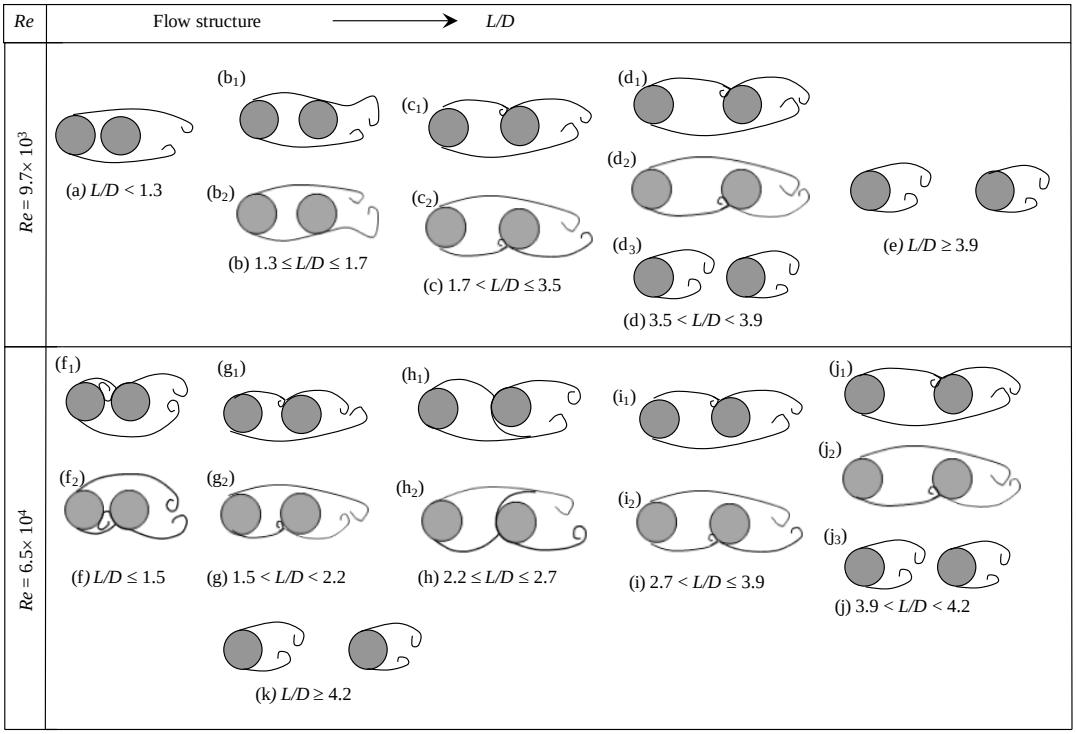

Fig 6. Flow structure with variation in *Re* and *L/D*. (a) Over-shoot, (b) rear-side reattachment, (c) front-side reattachment, (d) bi-stable between front-side reattachment and co-shedding flows, (e) co-shedding, (f) reverse-flow reattachment, (g) front-side reattachment, (h) front reattachment, (i) front-side reattachment, (j) co-shedding.

The power spectrum results at $Re = 1.6\times10^4$ (Fig 3) are almost the same as those at $Re = 9.7\times10^3$. Here the rear-side reattachment flow regime is shorter, $L/D = 1.3 \sim 1.5$. The bi-stable flow occurs at a smaller $L/D = 3.6$.

Results at $Re = 3.2\times10^4$ and 6.5×10^4 (Figs 4, 5) are similar, but completely different from those at $Re = 9.7\times10^3$ and 1.6×10^4. Therefore flow structures are presented for $Re = 6.5\times10^4$ only (Fig 6f-k). At $Re = 6.5\times10^4$, three *St* are seen for $L/D \le 1.5$. The first *St* is connected to the vortex shedding, while the second and third *St* are second and third super-harmonics of the first one. The corresponding flow structures (Fig 6f) explains why the second and third super-harmonic *St* exist for this *L/D* range. While for the front-side reattachment flow at $Re = 9.7\times10^3$ the shear reattaching on the cylinder splits into two and the high velocity slice of the shear layer goes to the downstream (Fig 6c), that at $Re = 6.5\times10^4$ the shear reattaching on the cylinder splits into two and the high velocity slice of the shear layer goes to the upstream and reattach again onto the rear surface of the upstream cylinder (Fig 6f). At $L/D = 1.5 < L/D < 2.2$, where only one peak is seen (Fig 5), the high velocity slice again goes on the same side to the downstream (Fig 6g). The high velocity slice goes on the other side passing over front surface at $2.2 \le L/D \le 2.7$, hence the two shear layers provide a strong alternating approaching flow on the downstream cylinder (Fig 6h), hence two peaks prevail in the power spectra (Fig 5). The flow structure generates a large C_{Lf} on the downstream cylinder, which will be shown later. With further increasing in *L/D*, the downstream cylinder acts as a stabilizer reducing the curvature of the upstream cylinder, the shear layer again reattaches with the high velocity slice passing on the same side (Fig 6i), hence a single peak is seen in the power spectra at $2.7 < L/D \le 3.9$ (Fig 5). The bistable flow occurs at $L/D = 4.0$, followed by a co-shedding flow at $L/D \ge 4.2$.

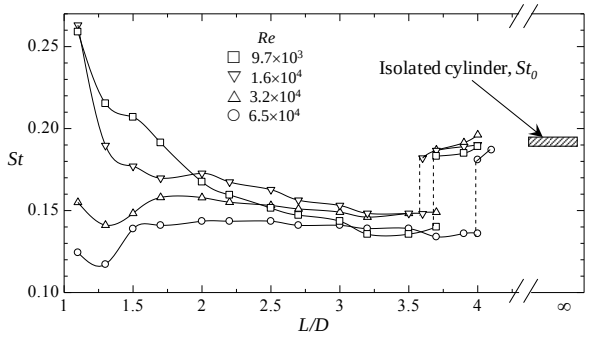

Fig 7. Dependence of Strouhal number (*St*) on *Re* and *L/D*

Fig 7 illustrates the trend of *St* with variation of *L/D* for the four *Re*. The dashed line represents the critical spacing. Isolated cylinder Strouhal number (St_0) range is also given for the *Re* range examined. The effect of *Re* on *St* is different at different *L/D*. For $L/D < 2$, *St* decreases with *Re*, but for $L/D = 2 \sim 3.5$, *St* augments for $Re = 9.7\times10^3$ to 1.6×10^4, then wanes for $Re = 1.6\times10^4$ to 6.5×10^4. Comparing Figs 6 and 7, it is seen that an over-shoot flow corresponds to *St* higher than St_0, a rear-side reattachment flow and co-shedding flow communicate a *St* equal to St_0, and front-side reattachment flow results in a *St* smaller than St_0.

3.2. Fluctuating Forces

Fluctuating drag and lift coefficients (C_{Df}, C_{Lf}) are presented in Figs 8 and 9. Both C_{Df} and C_{Lf} are very high

at $Re = 6.5\times10^4$, decreasing with decreasing *Re*. They are enhanced around $L/D = 1.4$ and 2.4, corresponding to the front-side reattachment flow where the high velocity slice of the shear layer goes to upstream or other side passing over the front surface (Fig 6f, h). Two peaks are formed at $Re = 3.2\times10^4$ and 6.5×10^4 but not at $Re = 9.7\times10^3$ and 1.6×10^4. It has been discussed in the introduction that a 'kink' in C_D profile with L/D exists at $Re < 3.1\times10^4$ and vanishes at $Re < 3.1\times10^4$. That is, the second peaks in C_{Df} and C_{Lf} are connected to the 'kink'. C_{Df} and C_{Lf} at $L/D = 2.4$ (second peak) are 2.8 and 2 times higher, respectively, than those for an isolated cylinder. Alam et al. [5] proved that near the peak ($L/D = 2.4$) the shear layers reattached on the downstream cylinder at a smaller angle of incidence on the front surface ($\theta = 55°$), producing a stronger Karman vortex behind the cylinder. Reattachment for other L/D occurred on the front-side surface. Even C_{Lf} of an isolated cylinder is also a strong function of *Re* because of the change in the formation length and transition position in the shear layers. Beyond the critical spacing, the cylinder experiences much higher C_{Df} and C_{Lf} resulted from the alternating Karman vortices from the upstream cylinder.

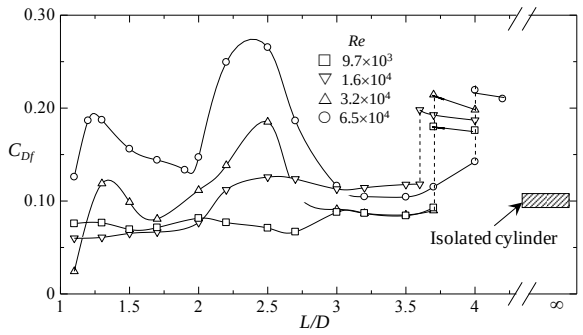

Fig 8. Dependence of fluctuating drag (C_{Df}) on *Re* and *L/D*

3.3. Physical Insight into *Re* Effect

St is dependent on reattachment position, formation length, wake width, etc. A flow structure map displaying how the flow structure vary with *Re* and *L/D* is given in Fig 10.

St at $L/D < 2$ drops monotonically with increasing *Re*, which is attributed to a decrease in the vortex formation length. In a single cylinder wake, the formation length reduces rapidly from $2.7D$ at $Re = 2.0 \times 10^3$ to $0.8D$ at $Re = 6.5 \times 10^4$ (Fig 11) and remains unchanged up to 2.0×10 [9]. A shorter length corresponds to a lower *St* and vice versa. Since the formation length of the upstream cylinder shear layer retreats with increasing *Re*, the rollup of the overshooting shear layers (Fig 6a) occurs near and eventually reattach on the downstream cylinder (Fig 6b), producing a drop in *St*. Since the downstream cylinder is completely submerged in the recirculation region of the upstream cylinder wake, a larger L/D implies a longer after-body length of the combined body and hence a reduced *St* in $1.3 \le L/D \le 1.7$. A wider wake corresponds to a smaller *St* and vice versa. A shear layer reattaching on the front-side of the cylinder is diverted away from the centerline, resulting in a wider wake and a lower *St*.

Transition in the shear layer being another important parameter plays a role in the modification of flow structure and hence of forces and *St*. For an isolated cylinder, transition length measured from the center of the cylinder decreases rapidly from $1.4D$ to $0.2D$ (Fig 11) when *Re* increases from 2.0×10^3 to $Re = 6.5 \times 10^4$ [9]. This explains why over-shot flow or rear-side reattachment flow occurs at low *Re* ($= 9.7\times10^3$ to 1.6×10^4) but not at higher *Re* ($=3.2\times10^4$ to 6.5×10^4, Fig 6). It has been shown that *St* is highly dependent on *Re* for $L/D < 2$ but not so much for $L/D > 2$. This is due to the fact that the upstream shear layer transition happens around the downstream cylinder for $L/D < 2$, moving from the downstream to the upstream with *Re*, hence the reattachment position as well, while that occurs much upstream of the downstream cylinder for $L/D > 2$. C_{Df} and C_{Lf} vary a lot with *Re* even for the $L/D > 2$. Reattachment position and incidence angle of the shear layer on the cylinder are responsible for this variation. Since transition happens between the cylinders, reattachment position and angle of incidence on the cylinder vary significantly with *Re*.

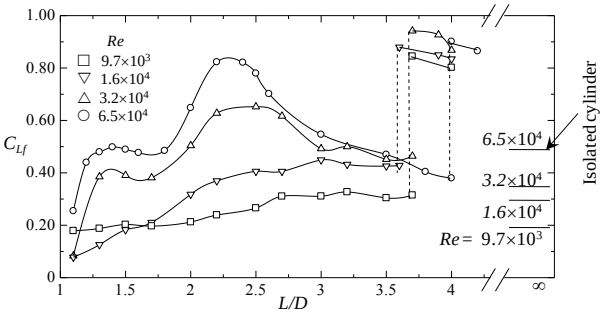

Fig 9. Dependence of fluctuating lift (C_{Lf}) on *Re* and *L/D*

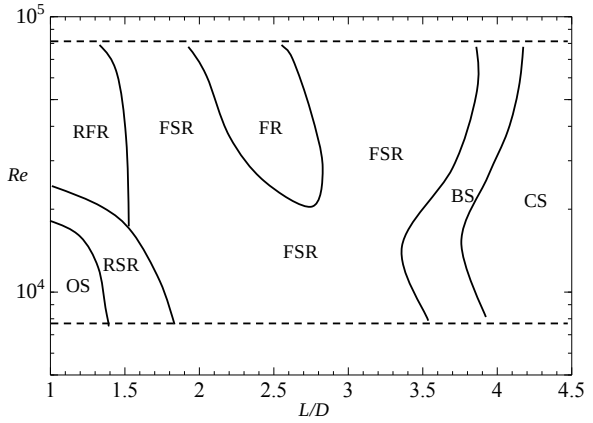

Fig 10. Flow structure with variation in *Re* and *L/D*. Over-shoot : OS; rear-side reattachment : RSR; front-side reattachment : FSR; front reattachment : FR; reverse-flow reattachment : RFR; bi-stable : BS; co-shedding : CS.

4. CONCLUSIONS

The paper leads to the following conclusions.

(i) C_{Df}, C_{Lf} and *St* are strong functions of *Re*. With increasing *Re*, while transition in the shear layers dominantly plays a role in changing flow structures, C_{Df}, C_{Lf} and *St* at smaller L/D (< 2), reattachment position and incidence angle of the shear layer on the downstream cylinder are responsible for the *Re* effect at larger L/D (> 2). *St* diminishes, and C_{Df} and

C_{Lf} augment with increasing *Re* for the *Re* range examined.

(ii) With increasing *L/D*, flow structure at $Re = 9.7\times10^3$ and 1.6×10^4 changes as over-shoot, rear-side reattachment, front-side reattachment, bi-stable and co-shedding, while that at $Re = 3.2\times10^4$ and 6.5×10^4 changes as reverse-flow reattachment, front reattachment, front-side reattachment, bi-stable, and co-shedding.

(iii) The 'kink' in C_D distribution obtained in the literatures or peak in C_{Df} and C_{Lf} at $Re = 3.2\times10^4$ and 6.5×10^4 is connected to front-side reattachment flow where the high-velocity slice of the shear layer reattaching on the downstream cylinder goes to the other side of the cylinder.

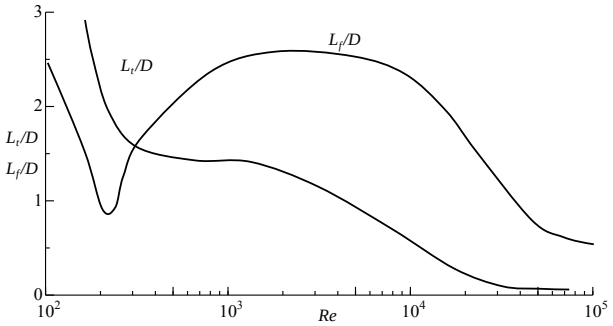

Fig 11. Vortex formation length (L_f) and shear-layer transition length (L_t) in terms of *Re* for an isolated cylinder [9].

5.ACKNOLEDGEMENT

M.M. Alam wishes to acknowledge support given to him by NRF through grant no A0U368, UP RDP through Grant No. AOT366, UP Research and Innovation Support through grant no AOS971. Professor Hiroshi Sakamoto, Kitami Institute of Technology, is also acknowledged for giving opportunity to conduct this experiment.

6.REFERENCES

1. Zdravkovich, M.M., 1987, "The Effects of Interference between Circular Cylinders in Cross Flow", Journal of Fluids and Structures 1: 239-261.
2. Alam, M.M. and Sakamoto, H., 2005, "Investigation of Strouhal Frequencies of Two Staggered Bluff Bodies and Detection of Multistable Flow by Wavelets", Journal of Fluids and Structures 20(3):425-449.
3. Biermann, D. and Herrnstein, Jr., 1933, "The Interference Between Struts in Various Combinations," National Advisory Committee for Aeronautics, Tech. Rep. 468.
4. Zdravkovich, M. M., and Pridden, D. L., 1977, "Interference Between Two Circular Cylinders; Series of Unexpected Discontinuities", Journal of Industrial Aerodynamics 2:255-270.
5. Alam, M.M., Moriya, M., Takai, K. and Sakamoto, H., 2003, "Fluctuating Fluid Forces acting on Two Circular Cylinders in a Tandem Arrangement at a Subcritical Reynolds Number", Journal of Wind Engineering and Industrial Aerodynamics 91:139–154.
6. Igarashi, T., 1984, "Characteristics of the Flow around Two Circular Cylinders Arranged in Tandem (2nd Report)", Bulletin of the Japan Society of Mechanical Engineers 27:2380–2387.
7. Ljungkrona, L., Norberg, C. H. and Sundén, B., "Free-Stream Turbulence and Tube Spacing Effects on Surface Pressure Fluctuations for Two Tubes in an In-Line Arrangement", Journal of Fluids and Structures 5,: 701-712.
8. Alam, M.M., Sakamoto H. and Zhou, Y., 2005, "Determination of Flow Configurations and Fluid Forces acting on Two Staggered Circular Cylinders of Equal Diameter in Cross-Flow", Journal of Fluids and Structures 21:363-394.
9. Zdravkovich, M. M., 1997, "Flow around circular cylinders. Volume 1: Fundamentals", Oxford Science Publications.

7. MAILING ADDRESS

Md. Mahbub Alam
Department of Mechanical and Aeronautical Engineering
University of Pretoria
Pretoria 0002, South Africa
Email: alam.mahbub@up.ac.za; alamm28@yahoo.com